Organic Electronics
Volume 10, Issue 4, July 2009, Pages 729-734

doi:10.1016/j.orgel.2009.02.027
Cite or Link Using DOI

Letter

Channel width effect for organic thin film transistors using TIPS-pentacene employed as a dopant of poly-triarylamine

Jae-Hong Kwon[a], Sang-Il Shin[a], Jinnil Choi[a], Myung-Ho Chung[a], Tae-Yeon Oh[a], Kyung-Hwan Kim[b], Min Ju Cho[b], Kyu Nam Kim[b], Dong Hoon Choi[b] and Byeong-Kwon Ju[a, c]

[a]Display and Nanosystem Laboratory, College of Engineering, Korea University, Anam-dong, Seongbuk-gu, Seoul 136-713, Republic of Korea

[b]Department of Chemistry, Korea University, Anam-dong, Seongbuk-gu, Seoul 136-713, Republic of Korea

[c]School of Electrical Engineering, College of Engineering, Korea University, Anam-dong, Seongbuk-gu, Seoul 136-713, Republic of Korea

Received 20 November 2008; revised 17 February 2009; accepted 26 February 2009. Available online 18 March 2009.

Organic Electronics 10 (2009) 729–734

Contents lists available at ScienceDirect

Organic Electronics

journal homepage: www.elsevier.com/locate/orgel

Letter

Channel width effect for organic thin film transistors using TIPS-pentacene employed as a dopant of poly-triarylamine

Jae-Hong Kwon [a], Sang-Il Shin [a], Jinnil Choi [a], Myung-Ho Chung [a], Tae-Yeon Oh [a], Kyung-Hwan Kim [b], Min Ju Cho [b], Kyu Nam Kim [b], Dong Hoon Choi [b], Byeong-Kwon Ju [a,c,*]

[a] Display and Nanosystem Laboratory, College of Engineering, Korea University, Anam-dong, Seongbuk-gu, Seoul 136-713, Republic of Korea
[b] Department of Chemistry, Korea University, Anam-dong, Seongbuk-gu, Seoul 136-713, Republic of Korea
[c] School of Electrical Engineering, College of Engineering, Korea University, Anam-dong, Seongbuk-gu, Seoul 136-713, Republic of Korea

ARTICLE INFO

Article history:
Received 20 November 2008
Received in revised form 17 February 2009
Accepted 26 February 2009
Available online 18 March 2009

PACS:
85.30.Tv
64.75.Bc
72.20.Fr

Keywords:
Organic thin film transistor
6,13-Bis(triisopropyl-silylethynyl)-pentacene
Poly-triarylamine
Channel width effect

ABSTRACT

The effects of the physical channel width on the characteristics of organic thin film transistors (OTFTs), made with 6,13-bis(triisopropyl-silylethynyl)-pentacene (TIPS-pentacene) embedded into poly-triarylamine (PTAA, hole conductor within an active channel), have been examined in this paper. The devices are estimated by measuring the drain-source current (I_{DS}) for different contact metals such as Au and Ag, at fixed gate and drain voltages. The results show that the threshold voltage (V_T) and I_{DS} increase with increasing channel width. Furthermore, it has been observed that the field effect mobility is dependent on V_T, which is influenced by the channel width. The OTFTs, produced using Au and Ag contacts, exhibited the highest values of mobility in the saturation regime, namely 5.44×10^{-2} and 1.33×10^{-2} cm^2/Vs, respectively.

1. Introduction

Electronics based on organic thin film transistors (OTFTs) have attracted much attention in recent years. This interest can be attributed to the emerging demands in electronic devices, such as radio frequency tags (wireless transponders) and smart cards, display (active and passive) media, and large area sensor arrays [1–4] on inexpensive plastic substrates, so that flexible, unbreakable, and light-weight electronics are possible using OTFT. Moreover, these devices permit the capability of being processed from solutions, allowing large scale fabrication techniques, such as screen printing [5], ink jet printing [6], imprinting [7] and roll to roll processing [8].

The most basic parameters of an OTFT are the effective channel length (L) and the width (W) of a transistor, which optimize the device performances. These parameters play an important role in governing the characteristics of the device [9] and therefore it has become more and more essential to accurately determine the real sizes of the OTFT's geometry for the device analysis and process control. However, considerable progress has been made in recent years in improving the performance of OTFTs, yet many of the designs, materials, and process parameters influencing OTFT performances are still poorly understood and not adequately controlled. Moreover, only little work

* Corresponding author. Address: School of Electrical Engineering, College of Engineering, Korea University, Anam-dong, Seongbuk-gu, Seoul 136-713, Republic of Korea. Tel.: +82 2 3290 3237; fax: +82 2 3290 3791.
E-mail address: bkju@korea.ac.kr (B.-K. Ju).
URL: http://diana.korea.ac.kr (B.-K. Ju).

1566-1199/$ - see front matter © 2009 Elsevier B.V. All rights reserved.
doi:10.1016/j.orgel.2009.02.027

surrounding the channel width effect has been carried out in field effect transistors based on metal oxide silicon [10], poly-crystalline silicon [11], or hydrogenated amorphous silicon [12] and thus the channel width effects on the OTFT's performance are not well known at the present time.

This work focuses on the three issues as follows: (1) thin film study of 6,13-bis(triisopropyl-silylethynyl)-pentacene (TIPS-pentacene) with semiconducting polymer binder (poly-triarylamine, PTAA) in order to impose a function as forming a good interfacial contact between the organic semiconductor (OSC) and the source/drain electrodes; (2) employing two kinds of metals, one with a low work function (Ag) and the other with a high work function (Au), in order to compare the function of metallurgy for low cost devices; and (3) a structural study of the channel dimension in order to optimize the device parameters effectively and to obtain good performance of the device characteristics.

2. Experimental

Fig. 1c shows a schematic diagram of the OTFT structure where an insulator layer of silicon dioxide (SiO_2) is thermally grown on top of a heavy doped p-type Si wafer to act as the gate contact. A highly doped p-type Si wafer was used both as a substrate and as a gate electrode for the bottom-contact structure. Initially, the gate insulator, for most of the devices, was thermally grown to a thickness of 100 nm. Sequentially, a 200 nm-thick source-drain Au and Ag contacts were fabricated on top of the insulator by a thermal evaporation method (DOV Co., Ltd) to give the channel widths in the range of 500–2500 μm, and the channel length of 100 μm using a shadow mask. Particularly, the source-drain interdigitatd finger (SDIF) type electrode were employed in our device configuration since this SDIF pattern permits the use of printing and other techniques for fabricating display backplanes that are not capable of attaining the fine resolution limits of standard silicon processing using photolithography. Next, the TIPS-pentacene mixed with PTAA were deposited by a drop casting from a 2 wt% solution of TIPS-pentacene in monochlorobenzene. Fig. 1a and b exhibit the molecular structures of TIPS-pentacene and PTAA, respectively. In our sample, PTAA was employed as a dopant and TIPS-pentacene was used as a host material. Also, in order to improve device performance, polymer binder, PTAA was employed to fabricate OTFT device with organic soluble TIPS-pentacene for decreasing the injection barrier from the metal electrode to the OSC and used as a hole conductor between the OSC and source-drain contacts for reducing the surface dipoles [13]. Here, TIPS-pentacene was synthesized following the procedure reported by our previous study [14]. PTAA was synthesized by following the literature method and a modified method [15–18]. All reactions were performed under an argon atmosphere unless otherwise stated. Finally, after coating the OSC, the device was annealed using a hotplate at 110 °C for 1 min.

The optical absorption spectra of the host-guest (TIPS-pentacene-PTAA) system film was obtained uisng UV spectrometry (Ultraviolet–visible, UV–vis, HP 8453, PDA, type λ = 190–1100 nm). The surface morphology of the OSC lay-

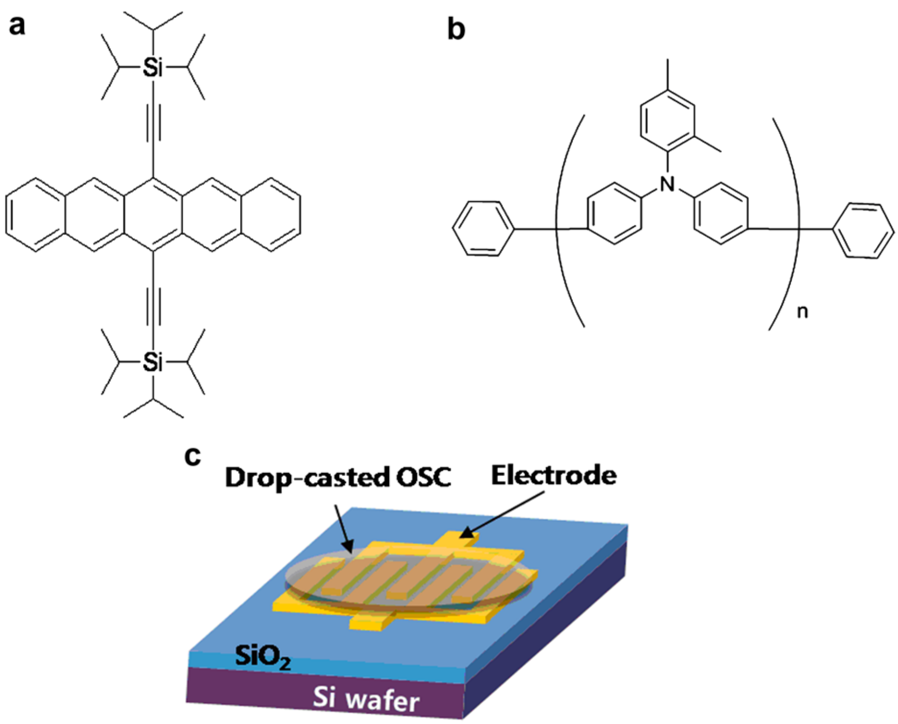

Fig. 1. The molecular structure of (a) TIPS-pentacene, (b) PTAA and (c) the schematic geometry of the OTFT on heavy doped silicon wafer with SDIF bottom contacts varying the *W*/*L* ratio from 25 down to 5 (channel length: 100 μm).

ers was observed using an AFM (XE-100 system). The transistor characteristics were measured using a Keithley SCS/4200 in a dark box.

3. Result and discussion

Fig. 2a shows the optical absorption spectra of the host-guest (TIPS-pentacene-PTAA) system film. Each spin-coated thin film (1 wt% solution) was formed by using the monochlorobenzene solvent. OSC films with 1:1 or 10:1 weight ratio mixture of TIPS-pentacene and PTAA were measured individually before and after the annealing process, as shown in Fig. 2a. The spectrum of TIPS-pentacene shows the crystalline properties, confirmed by the baseline floating phenomenon. When preparing the thin film without polymer binder, the quality of the surface of OSC was not well defined. Whereas, after mixing PTAA with a proper concentration, we could obtain much better film forming property. Therefore, the OSC was prepared with TIPS-pentacene and PTAA for improving film forming properties in a large area using the host-guest system, which produces a better film condition than the OSC without the polymer binder. Additionally, as it can be observed from the spectrum of Fig. 2a, the crystalline properties of the OSC film with 1:1 (TIPS-pentacene:PTAA) is not relatively lower than that with 1:10 (TIPS-pentacene:PTAA).

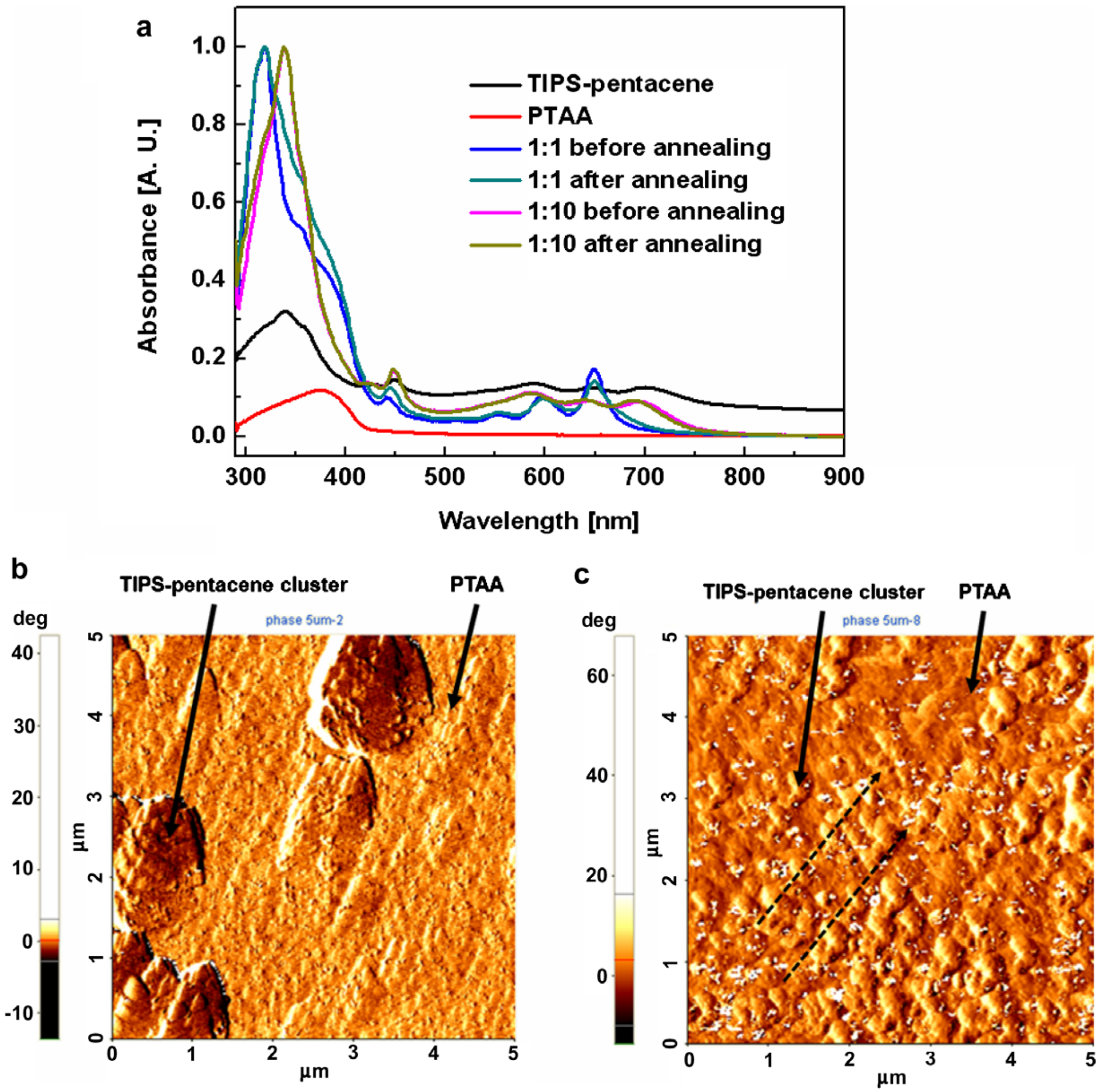

Fig. 2. (a) UV–vis spectra of thin films of spin-coated TIPS-pentacene (black), PTAA (red), OSC (TIPS-pentacene: PTAA = 1:1) film before annealing (blue), OSC (TIPS-pentacene: PTAA = 1:1) film after annealing (dark cyan), OSC (TIPS-pentacene: PTAA = 10:1) film before annealing (magenta), and OSC (TIPS-pentacene: PTAA = 10:1) film after annealing (dark yellow), individually. AFM images of OSC films for 1:1 (b) and 10:1 (c) weight ratio mixture of TIPS-pentacene and PTAA, respectively, after annealing. Scan size: 5 µm × 5 µm. (For interpretation of the references to color in this figure legend, the reader is referred to the web version of this article.)

Fig. 2b and c shows AFM (atomic force microscope) images of the OSC films for 1:1 and 10:1 weight ratio mixtures of TIPS-pentacene and PTAA after annealing, respectively. Bright areas in the images indicate higher values of the film thickness. Fig. 2b is a topographic image of the OSC film with 1:1 (TIPS-pentacene: PTAA) that shows discontinuous ~1 μm-TIPS-pentacene clusters, while Fig. 2c is the OSC film with 10:1 (TIPS-pentacene: PTAA) that shows continuous OSC film with regularly formed 20–30 nm-TIPS-pentacene clusters. It was clearly seen that the surface film showed straight line without any preferential orientation (dotted arrow in inset of Fig. 2c). Although good film has been obtained using the polymer binder, as shown in Fig. 2a, the TIPS-pentacene cluster can be a cause of poor carrier field effect mobility due to interference with the flowing carriers in the active channel. Therefore, the OSC (i.e., 10:1 weight ratio mixture of the TIPS-pentacene and PTAA) film, formed by drop casting a 2 wt% solution in monochlorobenzene, was prepared. As smaller concentration of polymer binder is used, the preferential orientation of TIPS-pentacene molecules is sustained on the surface of the blend film.

Fig. 3a and c shows the output characteristics of OTFTs with $L = 100$ μm and $W = 2500$ μm. The gate voltage (V_G) was increased in a stepwise manner from 0 V to −40 V for OTFTs with different electrodes of Au and Ag, respectively. Obviously, the output confirms typical characteristics of p-type OTFTs working in an accumulation mode. Fig. 3a and c shows that the drain-source current (I_{DS}) also saturates at an increasingly higher drain-source voltage (V_{DS}) with increasing V_G. However, the data in Fig. 3a and c shows that the linear and saturation regimes for each curve cannot be clearly distinguished, especially at high values of the gate bias, V_G, and when there is a lack of sat-

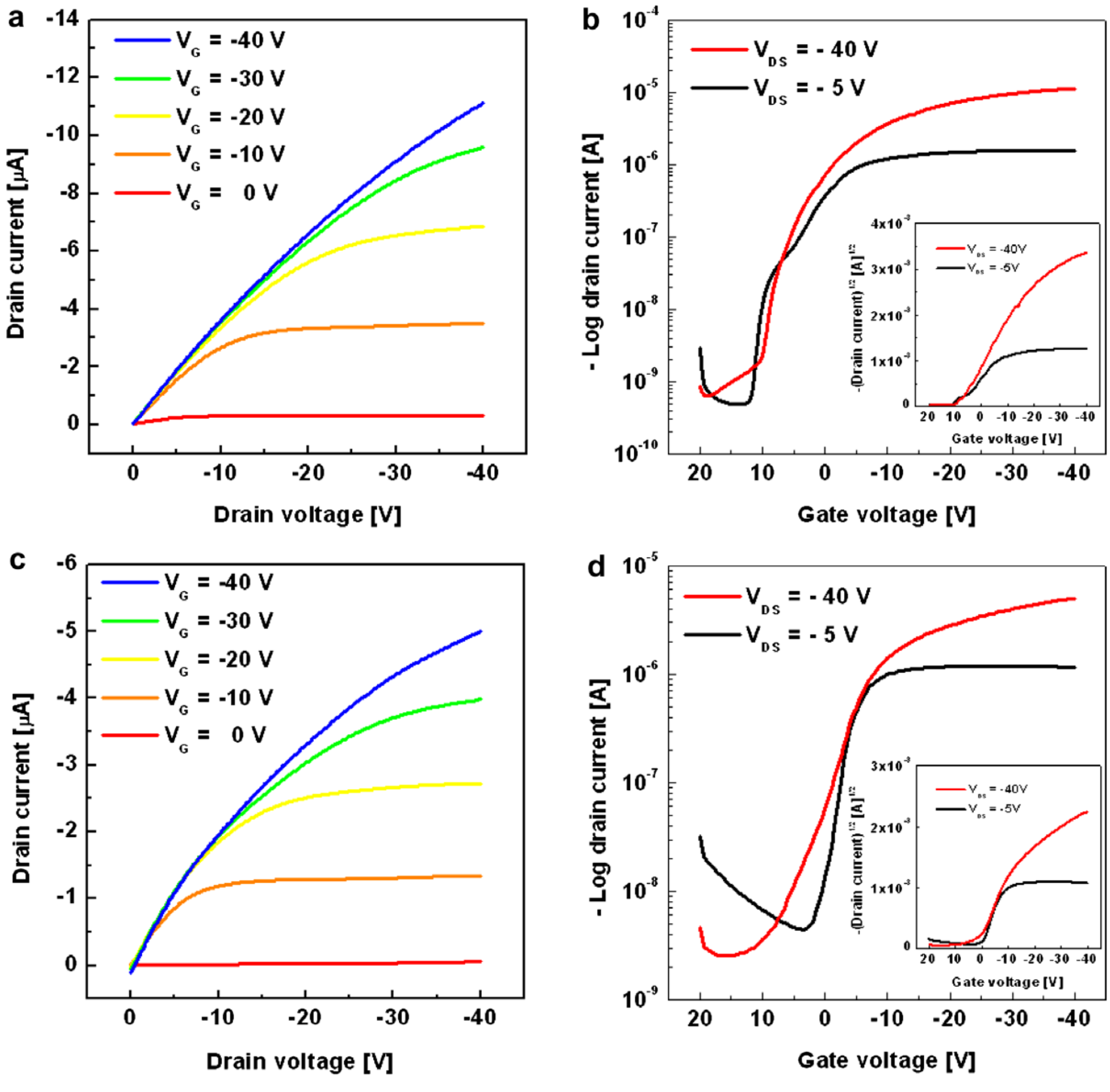

Fig. 3. Output characteristics I_{DS} vs. V_{DS} for OTFTs with different electrodes of Au (a) and Ag (c). Transfer characteristics $-log(I_{DS})$ vs. V_G and $-\sqrt{I_{DS}}$ vs. V_G (inset) measured for an OTFT ($W/L = 2500$ μm/100 μm) with Au contact (b) and Ag contact (d), respectively.

uration in I_{DS}. We believe this phenomenon, similar to the 'punch-through effect' [19] for the metal-oxide-semiconductor field effect transistor (MOSFET), which is caused by space charge limiting current [20], is preventing saturation.

Fig. 3b and d shows graphs of $-log(I_{DS})$ against V_G with their insets, $-\sqrt{I_{DS}}$ vs. V_G, for Au and Ag contacts, respectively. For each device, the carrier field effect mobility and the threshold voltage (V_T) were extracted in the linear ($V_{DS} = -5$ V) and saturation ($V_{DS} = -40$ V) regimes at a V_G of -40 V, where the results are shown in Fig. 4. Additionally, OTFTs with a channel length of 100 μm and a channel width range from 500 to 2500 μm were fabricated for different electrodes. However, all devices, regardless of their channel widths, exhibited a current on/off ratio between 10^4 and 10^5 for Au contacts, and between 10^3 and 10^4 for Ag contacts.

The data in Fig. 4 represent average values of device parameters such as field effect mobility and V_T when using Au and Ag electrodes. Here, we measured at least four devices to average the parameters for these plots.

In order to explore the effects of different source-drain electrodes on the performance of OTFTs, two kinds of electrodes having different work-functions were employed. Fig. 4 shows the transistor parameters of devices with Au and Ag electrode materials as source-drain contacts. It also shows the variation of carrier mobility and V_T as functions of the channel width W for devices with constant channel length $L = 100$ μm. The decreasing behaviors of carrier mobilities in both saturation and linear regimes with increase in channel width are observed from Fig. 4a and b, where the saturation mobility depended much more on the channel width than the linear mobility. Moreover, with increasing the channel width from 500 μm to 2500 μm, V_T is increased, as shown in Fig. 4c and d. These results, variation of carrier mobility and V_T as function of channel width, are in good agreement with previously reported work using inorganic TFT [11,12].

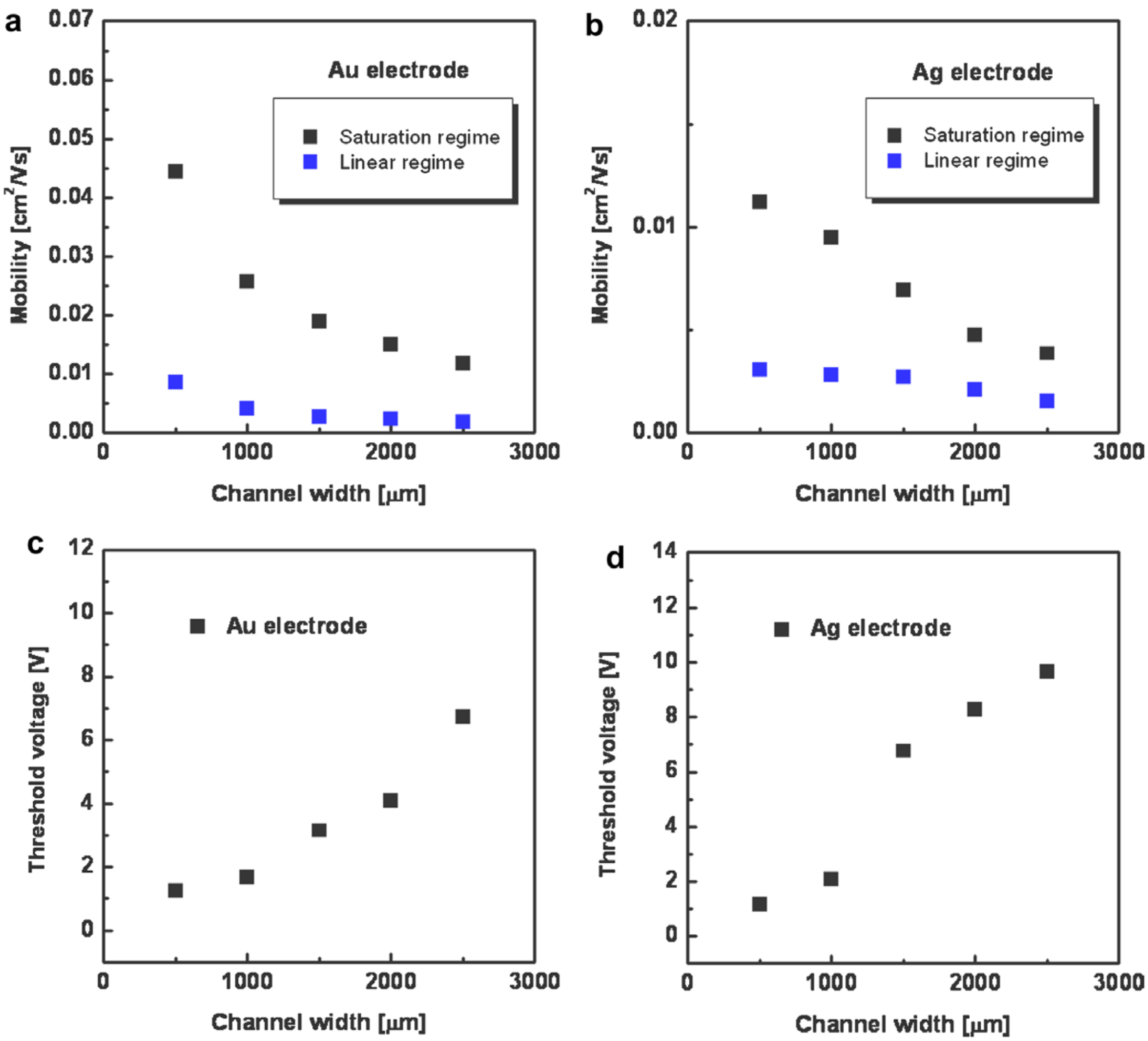

Fig. 4. Carrier field effect mobilities of Au contact (a) and Ag contact (b), and threshold voltage of Au contact (c) and Ag contact (d), extracted from the transfer characteristics. The channel widths range from 500 to 2500 μm; the channel length is 100 μm in all cases. The carrier mobilities were extracted at a V_G of -5 V and -40 V, respectively.

The field effect mobility increases with decreasing channel width, while V_T increases with increasing channel width in the saturation ($V_{DS} = -40$ V) and linear ($V_{DS} = -5$ V) regimes. Here, the I_{DS} of the devices increases with increasing channel width [10] since the transistor channel width to length ratio, which means larger I_{DS}, is proportional to the larger channel width. Although I_{DS} increases with increasing channel width [21], saturation and linear mobility reduce with increasing channel width since V_T increases. This, in turn, results not only in a significant increase in V_T but also in its pronounced channel width dependency.

4. Conclusion

In summary, in order to enhance device performance, TIPS-pentacene was employed as a host materials and a small amount of PTAA was used as a guest material. The host-guest system gave improved and uniform film formation in a large area, and helped the TIPS-pentacene to form a stronger binding between the source/drain electrodes onto the dielectric layer. Additionally, the devices were fabricated using different electrodes such as Au and Ag. Maximum saturation mobilities of 5.44×10^{-2} and 1.33×10^{-2} cm^2/Vs for OTFTs were obtained using Au and Ag contacts, respectively. From these results, it can be predicted that Ag-based devices would be expected to provide dramatic reductions in cost and to significantly improve the device performance upon full optimization. Finally, experimental observations showed that the field effect mobility depends on V_T. Although the field effect mobility values should increase as I_{DS} is proportionally increased, by increasing channel width, decrease in mobility were observed since V_T also increased.

Acknowledgements

This work was supported by the National Research Laboratory (NRL, No. R0A-2007-000-20111-0) Program of the Ministry of Education, Science and Technology (Korea Science and Engineering Foundation, KOSEF), the KOSEF grant funded by the Korea Ministry of Education, Science and Technology (MEST) (No. R11-2007-045-01003-0) and the KRF Grant funded by the Korean Government (MOEHRD) (KRF-2007-511-D00099). Particularly, D.H. Choi acknowledges the financial support by 21st Century Frontier Research Program (2008–2009).

References

[1] R. Rotzoll, S. Mohapatra, V. Olariu, R. Wenz, M. Grigas, K. Dimmler, O. Shchekin, A. Dodabalapur, Appl. Phys. Lett. 88 (2006) 123502.
[2] K. Tsukagoshi, J. Tanabe, I. Yagi, K. Shigeto, K. Yanagisawa, J. Appl. Phys. 99 (2006) 064506.
[3] L. Zhou, A. Wanga, S.-C. Wu, J. Sun, S. Park, T.N. Jackson, Appl. Phys. Lett. 88 (2006) 083502.
[4] T. Someya, Y. Kato, T. Sekitani, S. Iba, Y. Noguchi, Y. Murase, H. Kawaguchi, T. Sakurai, Proc. Natl. Acad. Sci. USA 102 (2005) 12321.
[5] J.H. Kwon, S.H. Lee, B.K. Ju, J. Appl. Phys. 101 (2007) 104515.
[6] H. Sirringhaus, T. Kawase, R.H. Friend, T. Shimoda, M. Inbasekaran, W. Wu, E.P. Woo, Science 290 (2000) 2123.
[7] G. Leising, B. Stadlober, U. Haas, A. Haase, C. Palfinger, H. Gold, G. Jakopic, Microelectron. Eng. 83 (2006) 831.
[8] G.P. Crawford, Flexible Flat Panel Displays, John Wiley & Sons Ltd., 2005 (Chapter 21), p. 409.
[9] C.R. Kagan, P. Andry, Thin-film Transistors, Marcel Dekker Inc., 2003. Part I, p. 43.
[10] Y.R. Ma, K.L. Wang, IEEE Trans. Electron Dev. ED-29 (1982) 1825.
[11] Y.-C. Wu, T.-C. Chang, P.-T. Liu, C.-S. Chen, C.-H. Tu, H.-W. Zan, Y.-H. Tai, C.-Y. Chang, IEEE Trans. Electron Dev. 52 (2005) 2343.
[12] A.T. Hatzopoulos, N. Arpatzanis, D.H. Tassis, C.A. Dimitriadis, F. Templier, M. Oudwan, G. Kamarinos, IEEE Trans. Electron Dev. 54 (2007) 1265.
[13] N. Koch, J. Ghijsen, A. Elschner, R.L. Johnson, J.-J. Pireaux, J. Schwartz, A. Kahn, Appl. Phys. Lett. 82 (2003) 70.
[14] J.H. Kwon, J.H. Seo, S.I. Shin, K.H. Kim, D.H. Choi, I.B. Kang, H. Kang, B.K. Ju, IEEE Trans. Electron Dev. 55 (2008) 500.
[15] Z. Yu, S. Tan, Z. Yuan, Y. Zou, B. Fan, Y. Li, J. Mater. Sci. 42 (2007) 1325.
[16] C.-G. Wu, Y.-C. Lin, C.-E. Wu, P.-H. Huang, Polymer 46 (2005) 3748.
[17] J. Veres, S. Ogier, S. Leeming, B. Brown, D. Cupertion, Mater. Res. Soc. Symp. Proc. 708 (2002) BB 8.7.1.
[18] J.H. Kwon, S.I. Shin, K.H. Kim, M.J. Cho, K.N. Kim, D.H. Choi, B.K. Ju, Appl. Phys. Lett. 94 (2009) 013506.
[19] B.G. Streetman, S. Banerjee, Solid State Electronic Devices, fifth ed., Prentice Hall, New Jersey, 2000. p. 192.
[20] J.G. Lee, Y.G. Seol, N.-E. Lee, Thin Solid Films 515 (2006) 805.
[21] J.H. Kwon, J.H. Seo, S.I. Shin, B.K. Ju, J. Phys. D-Appl. Phys. 42 (2009) 065105.